Journal of Thermal Science Vol.31, No.2 (2022) 571−581

https://doi.org/10.1007/s11630-022-1452-9 **Article ID: 1003-2169(2022)02-0571-11**

Ignition Characteristics of Lean Coal Used a Novel Alternating-Current Plasma Arc Approach

YAN Gaocheng*

School of Electric Power, Civil Engineering and Architecture, Shanxi University, Taiyuan 030013, China

Abstract: In order to achieve the target of reducing oil consumption to zero for pulverized coal (PC) boiler in power plant, the paper developed a novel coal pulverized ignition approach, called as Alternating-Current plasma (AC plasma) ignition, with the advantages of excellent PC combustion behavior and longer electrode life-span. The scientific principle of how to generate the AC plasma arc was elaborated in detail. First, the experiments on life-span of electrodes inside AC plasma generator had been conducted, finding a workable way to extend its life-span beyond 530 hours. Second, a new AC plasma burner specifically designed for lean coal according to the principle of PC staged combustion had been illustrated with diagrams and then used to ignite the PC-air stream under four kinds of conditions with a varying AC plasma power from 150 kW to 300 kW, focusing on analyses of the influence of AC plasma power on combustion behaver, such as combustion temperature, carbon burnout rate as well as PC combustion regime. The following results showed that in the case of the power of the AC plasma was P=300 kW, a satisfied PC combustion process could achieved, with the average PC combustion temperature of about 940°C, combustion flame length of 6.3 m, and the total carbon burnout rate of up to 52.2%. In addition, about 80% of the nozzle outlet section was filled with bright flame, while 81% of the PC was in zone of the cylindrical flame regime. The PC combustion modes were changed repeatedly during the process of combustion, which went from homogeneous combustion mode at initial ignition stage to combined combustion mode and heterogeneous combustion mode at middle stage, finally to combined combustion mode at later stage. The research conclusion in this paper has proved that the AC plasma ignition approach is feasible and effective to ignite low-rank coal without the present of fuel oil.

Keywords: pulverized coal combustion, alternating-current plasma ignition, oil-free ignition, utility boiler start-up, combustion mode

1. Introduction

Fuel oil is a common auxiliary fuel for the coal-fired power plants, usually used to preheat the furnace to operating temperature in the period of boiler start-up and to improve the combustion stability when in the lower load operation. However, it would bring a serious problem of huge fuel oil consumption for power plants [1–3]. Liu et al. [1] introduced that about 100 t of fuel-oil would be consumed for starting-up of 300 MW utility boiler firing bituminous coal. Messerle et al. [3] showed that the annual consumption of fuel oil for start-up and support at thermal power plant in Russia was estimated on 5 million tons with the tendency of increase, and in

Received: Nov 30, 2020 AE: YANG Bin Corresponding author: YAN Gaocheng E-mail: yangaochengbox@163.com

Kazakhstan this amount was 1 million tons per year, nearly half of this amount was used for the coal flame support. In addition, the use of fuel oil in power plants brought environmental pollution problems [4, 5]. For example, in China, in order to prevent from equipment failure due to the deposition of unburned residue fuel-oil on the electrode plate, the electrostatic precipitator is prohibited to run at the same time when fuel oil is firing in the furnace, inevitably resulting excessive emission of dust. Concerns over the increasing economic costs of fuel-oil and the environmental pollution have spurred the interest in developing oil-saving ignition methods, such as tiny-oil ignition [6–8], oxygen-rich ignition [9–11] and direct current plasma (DC plasma) ignition [12–16], among which the DC plasma ignition has received preferred attention due to improvement in PC combustion and lower cost with zero consumption of fuel oil. Ju et al. [12] provided a comprehensive overview of the progress in the knowledge of the DC plasma assisted combustion in applications, chemistry, ignition and flame dynamics; it was showed that when going through the plasma arc, coal particles with an initial size of 50 to 100 micrometers experienced "heat shock" and disintegrated into fragments of 5 to 10 micrometers, which increased the reaction area of coal particles and accelerated burning velocity with 3 to 4 times. Messerle et al. [13] had fulfilled plasma gasification of high ash bituminous coal; the results indicated that the plasma arc was able to gasify the coal particles rapidly by means of its high-temperature more than 6000°C, this multiplied the quantity of volatile matters (CO, OH, CO_2, CN, H_2, NH, H^+, H^-, O^+, O^-, C^+, N_2, CH_4, C_6H_6 and others) released from coal particles, which not only made ignition of pulverized coal (PC) easier, but also decreased NOx emission. Ma et al. [14] simulated the combustion of PC flame ignited by the DC plasma; the results presented that plasma arcs greatly reduced the activation energy required for PC combustion, releasing volatiles rapidly within 10^{-3} seconds. Ibrahimoglu et al. [15] conducted a 3D numerical simulation of a downdraft plasma gasifier with plasma reactions; the results had shown that plasma could directly gasify PC by using its high temperature characteristics, and the yield of volatiles would rise by 20%–80% compared with the normal situation. Messerle et al. [16] studied the operation of the furnace at the conventional combustion mode and the DC plasma activation mode; the results revealed that the plasma activation of combustion influenced on thermal technical characteristics of the torch and decreased carbon loss and nitrogen oxides concentration at the furnace outlet. Belosevic et al. [17] presented the results of numerical simulation of processes in air-coal dust mixture duct with DC plasma system; application of the plasma system in utility boiler furnaces promised to achieve important savings compared with the use of heavy oil burners. However, in China, the further application of DC plasma ignition technology was restricted by two problems [15, 18]. The first one was inadequate capability to strongly ignite low-volatile coal, due to lower electric power of DC plasma generator, which was only 150 kW at most. The second one was that as the most important component in DC plasma ignition, the electrode was unsatisfactory in aspect of life-span, which was usually less than 200 hours.

In order to alleviate the deficiency of DC plasma ignition above, an Alternating-Current (AC) plasma ignition approach was proposed in this paper, which had developed a unique high-speed rotating plasma arc, not only prolonging electrode life-span, but also allowing electrode to operate with a larger rated current. The increased rated current worked with other factors to enlarge power of AC plasma up to 2 times than that of DC plasma.

This paper firstly introduced the generation process of AC plasma arc, with a detailed explanation on its idea about prolonging electrode life-span and about increasing plasma arc power. The novelty of this paper was that a new model on AC plasma ignition burner was developed and subsequently used to carry out a series of experiments of lean coal ignition. Furthermore, some novel analytical indexes, such as combustion regime classification as well as PC combustion mode, had been introduced to study the PC combustion process, which was a new way to understand the PC flame shape and PC combustion intensity. This paper also focused on the analysis for PC combustion temperature distribution and carbon burnout rate evolution under different conditions. In addition, the experiments on electrode life-span were also conducted to try to verify the merits of AC plasma and to obtain quantitative conclusions about it.

2. Working Principle of AC Plasma Ignition

2.1 AC Plasma arc generation process

The process of producing an AC plasma arc is illustrated in Fig. 1. The arc-control cabinet output an electrical signal with the frequency up to 2000 Hz and the voltage more than 10 000 V, called the arc-striking signal, to the front electrode and the rear electrode, breaking the gap these two electrodes to get discharging. The electric circuit between electrodes is closed, where the 380 V power supply starts discharging, generating an electric arc (not plasma arc) at this gap between two electrodes. And then the compressed gas (0.5 MPa) is injected into the gap by strongly rotation way to absorb the thermal energy from electric arc. When being heated up to above 6000°C, the compressed gas goes into plasma state (that is the fourth state for matter), called plasma arc, as shown in Fig. 2.

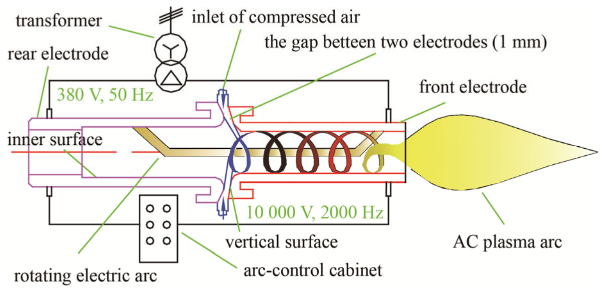

Fig. 1 Schematic diagram of arc generation process in AC plasma generator

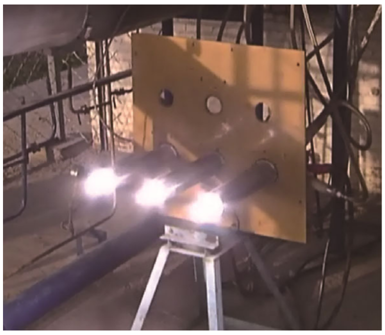

Fig. 2 The photo of AC plasma arc

AC plasma arc has two obvious advantages. The first one is longer life-span of electrode of AC plasma generator. The rotating compressed air forces the electric arc to rotate together along the inner surface of electrodes, not only avoiding the continuous erosion on a certain point by the electric arc, but also lowering the inner surface temperature of the electrodes. The second one is enlarged power of AC plasma generator. Thanks to success of decreasing inner surface temperature of the electrode during discharge, the allowable range of current I can be up to 500 A for AC plasma, higher than 300 A to 400 A for DC plasma. Also, under the condition that the voltage and current are equal, the AC power is 1.35 times in electric power than the DC power. To sum up, the AC plasma generator is usually more than twice as powerful as DC plasma generator, reaching up to 300 kW.

2.2 AC plasma burner

Different from the traditional method of igniting PC in the furnace by fuel oil during the boiler start-up, the AC plasma ignition approach aims to make PC ignite in special burner by AC plasma arc without the present of fuel oil. Hence, a novel construction of PC ignition burner equipped with three sets of AC plasma generators, called AC plasma burner, is invented, as shown in Fig. 3.

The AC plasma burner is composed of combustion sections I and II, gas-solid separators I and II (a stop block with a shape of ring), three sets of AC plasma generators, nozzle and cooling air shell. The three sets of plasma generators with a distance of 250 mm each other

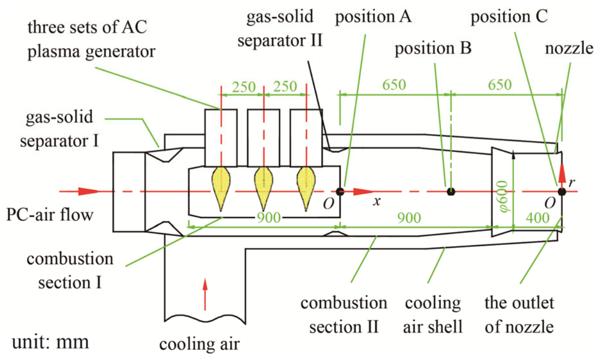

Fig. 3 Schematic diagram of AC plasma burner

are connected to the combustion section I; the nozzle is cylindrical in length of 400 mm and inner diameter of φ 600 mm, while the combustion section I is 900 mm in length as same as the combustion section II. The AC plasma burner works based on the theory of the staged PC combustion, which means all of PC is separated into three parts, namely the high concentration PC, the middle concentration PC and low concentration PC, and then they are ignited in sequence. Among them, only the high concentration PC is ignited by AC plasma arc, while the rest is fired by the heat energy released from the ignited high concentration PC. From there, the target to ignite as much PC as possible at minimal cost is realized. The detailed description is as follows. The PC is carried by primary air to the AC plasma burner inlet, where part of the PC collides with the gas-solid separator I. The collided PC alters its original trajectory to flow towards central zone of burner, where the PC concentration therefore gets rise, forming high concentration PC, accounting for about 30% of total PC. The high concentration PC flows into combustion section I, where it is subject to thermal shock from AC plasma arcs three times, then get ignited to release huge heat energy. The part of PC flowing outside of combustion section I collides with the gas-solid separator II, and then flows to central zone of combustion section II to form the middle concentration PC, making up 40% of total PC. The middle concentration PC is ignited by the combustion flame of high concentration PC, instead of AC plasma arc. The rest occupying 30% of total PC is low in concentration due to twice colliding separation and thusly called as low concentration one, which appears near to inner surface of burner. The low concentration PC is ignited by combustion flame of the high and middle ones before leaving away from nozzle. From there, it can be concluded that as long as the plasma ignites only 30% of the PC; the goal of igniting all of that can be achieved, which is important for either reducing ignition costs or enlarging the capacity of igniting more PC. Besides, to prevent the burner from overheating, the cooling air with 3500 Pa is introduced to cool the outer surface of combustion section II and nozzle, which is proved to be capable to keep the temperature of burner less than 250°C in operation.

Three ports are available on the burner for measure and sampling purpose, respectively marked as position A, position B, and position C. Among them, position A is at the outlet of combustion section I, position C at the outlet of nozzle, while position B lays between position A and position C, and the length from position A to position B is 650 mm as same as that from position B to position C.

3. Experiments on Life-Span of AC Plasma Electrodes

3.1 Experimental scheme

In order to verify whether AC plasma has the advantage of prolonging life-span of electrode, as well as to give a quantitative conclusion, a series of experiments on life-span of AC plasma electrodes were carried out. To more intuitively understand the electrode operation process, a simplified schematic of electrodes was shown in Fig. 4. The electrode was made of red copper and surrounded by cooling water. The cooling water was introduced near the outlet of the front electrode, and then flowed to the rear electrode along the outer surface of the electrodes, finally leaving from the rear part of the rear electrode. In addition, a thermocouple with model of WRN230 with temperature range of –40°C to 800°C and permissible error of ±1.5°C was mounted on the outer surface near the front electrode outlet, where the electrode burn-through accident most likely happened, because that the temperature here was the maximum. Compressed air was fed into the inside of electrodes through a gap between the front and rear electrodes, and then being turned into plasma arc finally.

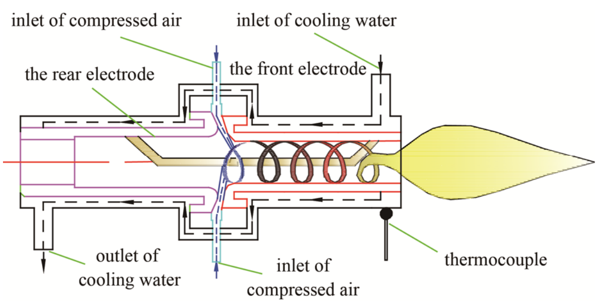

Fig. 4 Schematic on experiments of life-span of the electrodes of AC plasma generator

The electrodes were most likely damaged due to the electric corrosion from arcing current and the erosion from high temperature plasma arc. Therefore, the arcing current and the cooling water flow were consider as the two important factors to be experimentally studied in detail, while other parameters remained constant, as shown in Table 1.

Table 1 Operating conditions in experiments of life-span of the electrodes

Parameters	Condition
flow rate of cooling water Q_{water} /t·h^{-1}	4
cooling water pressure P_{water}/MPa	0.5
inlet temperature of cooling water T_{water}/°C	25
compressed air pressure P_{air}/MPa	0.5
volume flow rate of compressed air Q_{air}/Nm^3·h^{-1}	1.5

3.2 Experimental results and analysis

The experiments of the electrode life-span were conducted through four cases with different cooling water flow rates, named Case 1, Case 2, Case 3, and Case 4. For each case, the relationship of arcing current and electrode life-span was given in Fig. 5. To better understand the heat transfer process between electrodes and cooling water, the temperatures curves of outer surface of electrode were added.

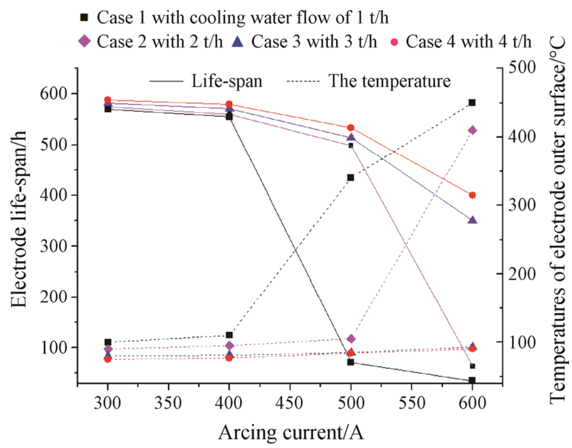

Fig. 5 Effects of cooling water flow and arcing current on life-span of electrode

It could be found from Fig. 5 that there were three points with abnormal short life-span on the life-span curves, all of which were correspond to the points with high temperature on the temperature curves. For example, for Case 1, when the arcing current was respectively equal to 500 A and 600 A, the electrode temperatures rose to 340°C and 450°C accordingly, while corresponding life-span rapidly went down to 71 h and 35 h. Similar phenomenon also occurred at position with arcing current of 600 A for Case 2, where the electrode temperature of 410°C corresponded to life-span of 64 h. From different perspectives, in the case that the temperature of electrode was low, the life-span was obviously longer, basically reaching more than 530 h. From there, it could be concluded that abnormal high temperature was main factor shrinking life-span. Furtherly, the reason for the temperature abnormity may be explained as follows. The saturation temperature of water was 151°C when P_{air} =0.5 MPa. Once being higher than the corresponding saturation temperature, the water would vaporize completely, along with a sharp decrease in thermal conductivity, resulting rapid increase in temperature of electrode. Therefore, we suggested that the cooling water flow rate should be increased until the surface temperature of the electrode was lower than its saturation temperature. Furthermore, through comparing the electrode surface temperature curve between Case 3 and Case 4, it could found that the influence of cooling water on the electrode life-span was not significant in the case the electrode temperature was lower than saturation temperature of cooling water, which indicated that the continued increase of cooling water flow rate could not significantly increase the electrode life-span under condition of no cooling water vaporization.

We could also found from Fig. 5 that the electrode life-span curves for Case 3 and Case 4 kept a slow decline along with the increase in arcing current when the arcing current ≤500 A, but they obviously faster got down when the arcing current >500 A, which means that the arcing current of 500 A was a turning point for the electrode life-span curve. So it was a wise choice to keep the arcing current below 500 A during operation.

Based on the above analysis, the AC plasma generators should be operated in such way that the outer surface temperature of the electrode should be monitored to prevent from the evaporation of cooling water, along with that the arcing current was tried to avoid more than 500 A.

4. Experiments on PC Ignition

4.1 Experimental set-up

The experimental set-up was composed of PC bunker, screw feeder, air compressor, switch cabinet, current-limited reactor, power transformer, arc-control cabinet, AC plasma burner, primary fan, cooling fan and combustion chamber, etc., as shown in Fig. 6.

The screw feeder was used to precisely control PC feeding quantity in range of 3–8 t/h. The air compressor produced compressed air with pressure of up to 0.6 MPa and volume flow rate of 3.2 m^3/min. The power transformer was used to lower the 6000 V bus voltage to 380 V to match the plasma generator. The arcing current was adjusted by the current limiting reactor. The switch cabinet was used to control main power supply and to provide electrical protection for whole electrical system, while arc-control cabinet was for controlling arc-striking power supply to produce a qualified arc-striking signal. Primary fan provided the primary air with presser of 4500 Pa to carry PC into burner, while the cooling air with 3500 Pa came from the cooling fan. The combustion chamber was a cuboid with total length of 10 m and high of 3.5 m and width of 3.5 m, on the side wall of which five measuring holes with spacing of 1000 mm were installed, numbered D1, D2, D3, D4 and D5 respectively. In each measuring hole, a thermocouple had been installed to test the temperature of the PC-air flow. The flue gas was firstly purified by the water spray device and then expelled out through chimney by an induced draft fan with presser of 3000 Pa. The operation parameters were shown in Table 2.

4.2 Experimental measurements

Double-Platinum rhodium thermocouple with the model of WRR-131 was used for measuring PC-air flow temperature, which was valid in range of 0–1600°C and less than ±0.5%*t* in relative error. Stainless steel water-cool probe used for sampling was composed of a water-inlet pipe, water-outlet pipe, sampling tube, outer pipe and supporting components. A sample of the high-temperature gas was collected into the sampling tube and then cooled by high pressure cool water of 0.5 MPa delivered through the water-inlet pipe and after

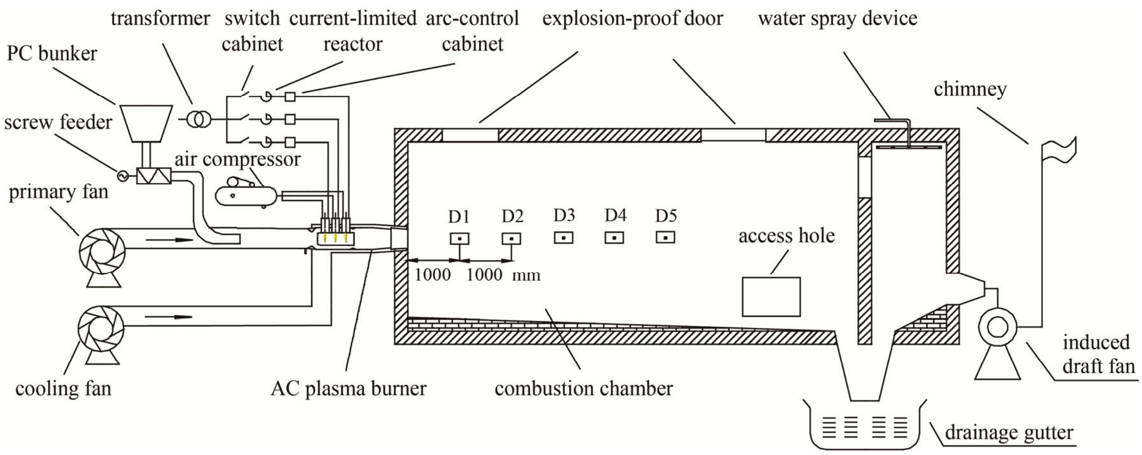

Fig. 6 System of AC plasma ignition experiments

Table 2 Operation parameters

Parameters	Operation values
Compressed air pressure P_{air}/MPa	0.5
Compressed air flow rate Q_{air}/m^3·min^{-1}	0.9
Primary air velocity v/m·s^{-1}	22
Primary air temperature T_{air}/°C	25
PC-feed rates Q_{PC}/t·h^{-1}	6
Voltage of the plasma generator U_{power}/V	380
Frequency of arc-striking signal f/Hz	2 000
Voltage of arc-striking signal U_{signal}/V	10 000

heat change flowed out via the water-outlet pipe. A water pump provided continuous water circulation. In order to make sure the PC flowed into sampling tube completely stop burning, the inner surface temperature of probe was remained less than 60°C by cooling water. The cooled flue gas then flowed into the splitter in which it was seperated to two parts: solid sample and net smoke sample. Net smoke sample was delivered by a pump into a Testo 350M gas analyzer for subsequent analysis. The accuracy of that analyzer for each species measurement was 1% for O_2 and 5% for CO. Solid samples was analyzed for its component, shch as FC (fixed carbon), V_{daf}, and A_{daf}. The analysis methods for V_{daf}, and A_{daf} were in accordance with GBT212-2008 Coal Industry Analysis Method of China national standard. FC content was calculated by means of FC=1–V_{daf}–A_{daf} (the moisture content of sample was considered as zero because that sample had been subjected to high temperature combustion). All measuring instruments had been calibrated before use.

4.3 Coal used in experiments

The coal used in the experiments was the lean coal in Jinzhong city, Shanxi Province, China, as shown in Table 3.

Table 3 Characteristics of lean PC used in the experiments

(a) Proximate analysis (as air dry basis)

Volatile matter /%	Ash	Moisture /%	Fixed carbon /%	Net calorific value /kJ·kg^{-1}	PC fineness R90 /%
15.8	22.4	5.8	56	21 000	15

(b) Ultimate analysis (as air dry basis)

Carbon /%	Hydrogen /%	Sulfur /%	Nitrogen /%	Oxygen /%
63.55	2.79	1.2	1.01	2.95

4.4 Experimental scheme

The power of AC plasma generator has essential influence on the PC ignition process. The target here is to study the combustion characteristics of lean coal when the power of AC plasma generator is varying over a large range, trying to find a desirable approach for application of AC plasma in lean coal boiler. Four representative experimental schemes, respectively named Case 5, Case 6, Case 7, Case 8, had been chosen. For these four cases, only the AC plasma generator power was different, varying from 150 kW to 300 kW, while the other parameters always kept constant to eliminate the influence on the coal combustion characteristics caused by variation of those parameters, as shown in Table 4.

Table 4 Experimental parameters

Experiment scheme mark	Case 5	Case 6	Case 7	Case 8
power of generator $P_{generator}$ /kW	150	200	250	300
arcing current I/A	225	300	380	450
primary air velocity v/m·s^{-1}	22	22	22	22
primary air temperature T_{air}/°C	25	25	25	25
PC-feed Q_{PC}/t·h^{-1}	7	7	7	7

4.5 Experimental results and analysis

The PC combustion process had been researched by combustion temperature, carbon burnout rate and PC combustion mode, focusing on analysis and comparison for PC combustion difference caused by the variation in AC plasma power.

4.5.1 PC combustion temperature

The PC combustion temperature (the combustion temperature here refers to the temperature of mixture of the PC and air in igniting process, tested by thermocouple) is the most important and intuitive to reflect the PC combustion regime. The PC combustion temperature was analyzed from two aspects as follow: the axial temperature distribution along the center line of combustion chamber and the radial temperature distribution at outlet of nozzle.

4.5.1.1 Axial temperature distribution

AC plasma generator power had a significant effect on PC combustion temperature, as shown in Fig. 7.

As could be seen from Fig. 5:

(1) Case 5 ($P_{generator}$=150 kW): The temperature curve was characterized by a continued decline in whole combustion process. The maximum temperature appeared at position A, only reaching T= 690°C, on one hand, which was higher than the devolatilization temperature of 450°C–500°C, indicating that the devolatilization process of the high concentration PC had happened in the combustion section I, on the other hand, which was lower than the lean coal-air flow ignition temperature of 840°C [19], showing that it was very difficult to make PC strongly burn.

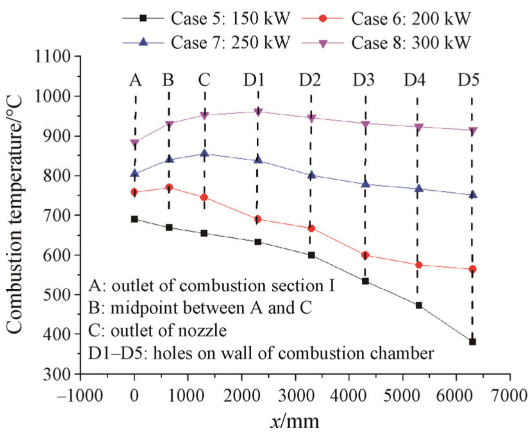

Fig. 7 Axial temperature distribution of PC-air flow along the center line of combustion chamber

(2) Case 6 ($P_{generator}$ =200 kW): A slight temperature ascent presented between position A and B, slowly rising from the 758°C at position A to 770°C at position B, but such combustion temperature level was not enough to ignite the FC component in PC. Therefore, volatiles combustion was dominating from position A to B where FC combustion was negligible. After flowing into combustion chamber, the PC-air flow underwent faster decrease in temperature, dropping to 564°C at the position D5. This may be caused by “cold furnace effect” which refers to a situation like this: as soon as flowing into the cold low-temperature boiler furnace, the burning PC-air flow will rapidly radiate out large of heat and convect with the cold air around it, resulting the destruction of combustion stability. The experiment results of Case 6 indicated that the AC plasma power of $P_{generator}$ =200 kW was of deficiency to ignite PC successfully.

(3) Case 7 ($P_{generator}$=250 kW): In the burner (i.e., from position A to C), the continued temperature ascend was observed, going up to the maximum value of 855°C at position C. The temperature profile indicated that not only the high concentration PC was strongly burning, but also the middle concentration PC was ignited by the high concentration PC flame. But after flowing into the chamber, the PC-air flow presented a modest decline in combustion temperature, keeping in the range of 750°C to 830°C. Such a temperature level only made the PC burn faintly, which was certainly not satisfactory from a boiler start-up point of view. Therefore, we could find that the case of $P_{generator}$=250 kW had not enough ability to offset the negative influence of “cold furnace effect”.

(4) Case 8 ($P_{generator}$ =300 kW): The combustion temperature at outlet of the combustion section I (i.e., position A) had gone up to 885°C, reflecting that the FC component had been ignited strongly in combustion section I. It could be found that the combustion temperature was on a continuous ascent inside of burner, reaching 954°C at position C, and the temperature curve kept near horizontal in whole chamber, from which we could make a conclusion that the case of $P_{generator}$ =300 kW was qualified to deal with the “cold furnace effect”. Average temperature in the chamber reached about 940°C, which was higher by about 20°C than that in burner. The max temperature value appeared at position D1, going up to 962°C. We had observed a bright golden PC flame filling the whole chamber, with the flame length of above 6.3 m, as shown in Fig. 8.

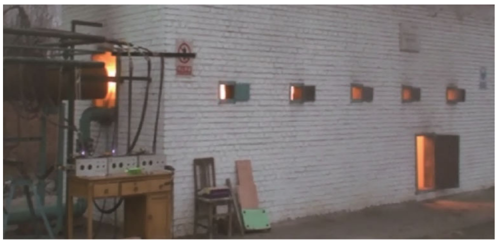

Fig. 8 Photo of PC combustion flame in Case 8

4.5.1.2 Radial temperature distribution

AC plasma generator power had a significant effect on radial temperature distribution, as shown in Fig. 9.

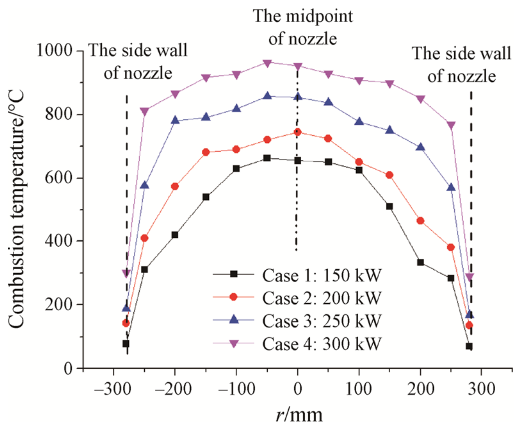

Fig. 9 Radial temperature distribution on the outlet of nozzle

Fig. 9 presents PC combustion temperature on the outlet of nozzle under different generator power, which could be used to judge the PC combustion regime by the method introduced in Ref. [19], the details were as follows: the combustion regime of coal particle group could be classified as four types: slight flash regime, normal flash regime, strip-shaped flame regime and cylindrical flame regime, among which the strip-shaped flame regime meant that the PC had been ignited but in a weak state, while the cylindrical flame regime represented a desirable PC combustion level. According to the data from Ref. [19], the lean PC-air flow would come to slight flash regime when up to 530°C, to normal flash regime when up to 620°C, to strip-shape flame regime when up to 730°C, and to cylindrical flame regime when up to 840°C. In addition, it was considered that there was no significant chemical combustion reaction happened if the lean PC-air flow temperature was lower than 530°C.

Based on the theory of combustion regimes above, the outlet of nozzle had been divided into five zones according to their temperature values, namely non-combustion reaction zone (T_{flame}<530°C), slight flash zone (530°C<T_{flame}<620°C), normal flash zone (620°C< T_{flame} <730°C), strip-shape flame zone (730°C<T_{flame} < 840°C) and cylindrical flame zone (T_{flame}>840°C). The quantity of PC in each of the five zones was calculated out based on an assumption that the PC concentration distribution was considered to be standard normal distribution. Finally, the ratio of the PC mass in individual zone to the total PC mass had been figured out, as shown in Fig. 10.

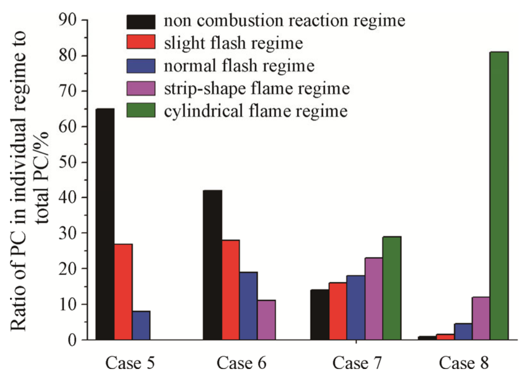

Fig. 10 Proportion of PC in different combustion regimes

As could be seen from Fig. 10:

(1) In Case 5: Neither strip-shape flame regime or cylindrical flame regime was observed. Up to 65% of the PC was in the non-combustion reaction regime, while only 8% of that was in the normal flash regime, which meant the PC was barely burning.

(2) In Case 6: The cylindrical flame regime still did not appear, and the PC in strip-shape flame regime only accounted for 11% of the total PC. Therefore it was concluded that the PC ignition was failure.

(3) In Case 7: The obvious improvement in the PC combustion intensity had been observed, with 29% of the PC in strip-shape flame regime and 23% in cylindrical flame regime, which showed that near half of the PC had been in a state of combustion. But it should be point out that about 14% of the PC was still in non-combustion reaction regime, which was unacceptable to power plant, because it meant to lose large coal energy and, more importantly, to increase the possibility of residual carbon reburning in boiler flue. So we considered that the PC combustion had not reached desirable level. It is necessary to furtherly increase the power of AC plasma generator.

(4) In Case 8: 81% of the PC was in the cylindrical flame regime, while 12% in strip-shape flame regime, and only 1.5% in the non-combustion reaction regime. As shown from Caes 4 curve in Fig. 9, the range full of strip-shape flame as well as bright flame regimes was –250 mm<r<240 mm, accounting for about 80% of the total area of the nozzle outlet (its radius r=300 mm). According to theory of the PC combustion regime that the strip-shape flame and bright flame regimes represent the success of PC ignition, it could be concluded that most areas of the nozzle outlet were full of the PC flame. Such conclusion also could be proved by the photo from Fig. 6, showing that the theory of the PC combustion regime was in good agreement with experimental results.

4.5.2 Carbon burnout rate

The burnout rate of carbon was analyzed by two parameters: the first one was the total burnout rate of carbon, which was the accumulated mass fraction of carbon burning out upstream of sampling position, representing the total PC combustion intensity; the second one was the local burnout rate of carbon, which was the mass fraction of carbon burning out between two adjacent sampling positions, representing the local PC combustion intensity in an individual zone. From there, it was convenient to reveal the change of PC combustion intensity and analyze those reasons.

The total burnout rate of carbon was calculated by Eq. (1) [20]:

$$\psi_i = \frac{1-\left(w_k / w_{xi}\right)}{1-w_k} \tag{1}$$

where ψ_i was the total burnout rate of carbon at position i, %; w_k was initial ash content in coal, %; w_{xi} was ash content in sample from position i, %;

The local burnout rate of carbon was calculated by Eq. (2):

$$\zeta_i = \psi_i - \psi_{i-1} \tag{2}$$

where ζ_i was the local burnout rate of carbon at position i, %; ψ_i was the total burnout rate of carbon at position i, % (seen in Eq. (1)).

Fig. 11 showed the evolution of local carbon burnout rate ζ and total carbon burnout rate ψ_i calculated by Eq. (2) along the center line of combustion chamber. It could be found that the local carbon burnout rate ζ was mainly affected by two factors: plasma arc and combustion temperature. The detailed analysis was as follows:

(1) The influence of plasma arc

Due to extremely high plasma arc temperatures (over 6000°C), the carbon in the PC was instantly ignited or even vaporized when passing through the plasma arc [21]. Plasma arc exhibited an inherent advantage in the aspect

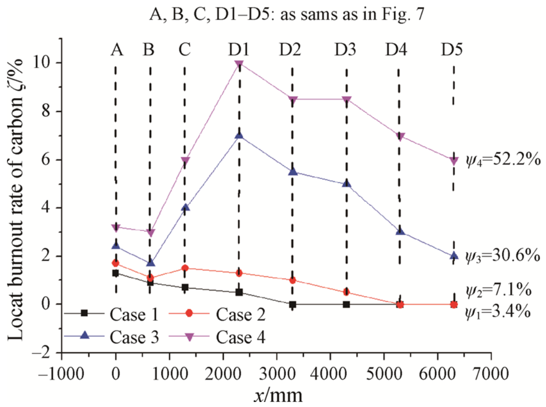

Fig. 11 Evolution of local carbon burnout rate at the center line of combustion chamber

of improving carbon burnout rate. Especially for AC plasma ignition system with three sets of plasma generators, this advantage worked better. For example, the local carbon burnout rates at position A were always higher than those at position B for all curves, even for Case 6 to Case 8 where higher temperature was at position B rather than position A, i.e. "though $T_A < T_B$, but $\zeta_A > \zeta_B$". This indicated that, at the initial stage of PC ignition, the plasma arc has higher influence on carbon burnout rate than temperature. However, because that PC passing through the plasma accounted for a tiny proportion of the total amount of PC, the local carbon burnout rate in the combustion section I was low, only reaching 2% for Case 4, which was the maximum local carbon burnout rate at position A in all four cases.

(2) Influence of combustion temperature

Combustion temperature is the most important factor influencing the carbon burnout rate. In general (except position A for Case 6 to Case 8), the burnout rates of carbon got up with the increase in combustion temperature. Especially when the combustion temperature was higher than the PC-air flow ignition temperature of 840°C, the ignited carbon particles amounts would go up greatly, making the local carbon burnout rate rise rapidly. For example, for Case 2 in which the combustion temperature was always lower than ignition temperature, its maximum local carbon burnout rate, appeared at position A, was as low as 1.7%, while for Case 3, the local carbon burnout rate significantly increased to a relatively high level, reaching 4% at position C and 7% at position D along with the PC-air flow temperatures over 840°C at position C and D.

In Case 4, as the combustion temperature between position A and position D5 all exceeded the ignition temperature of 840°C, the local carbon burnout rates reached the highest level in all experiments. The maximum local carbon burnout rate appeared at position D1, reaching 10%, followed by D2 and D3, all reaching 8.5%. Therefore, it was easy to find that the zone with the highest combustion intensity was from position C to position D3. Eventually, the total burnout rate of carbon reached 52.2%. Considering that the carbon burnout rate more than 50% was achieved just in a 6.3 m-long combustion space (the distance between position A and position D5 was 6.3 m), the combustion intensity of carbon particles was high enough to make a judgment that the PC was already in a stable combustion state.

4.5.3 Analysis on PC combustion mode

It is well known that PC combustion has three modes: homogeneous combustion, combined combustion and heterogeneous combustion. But it is extremely difficult to exactly estimate the PC combustion mode. Han et al. [19] introduced a method to assess the PC combustion mode by comparing the *V*/FC (*V* referred to volatile content of the sample, and FC represented fixed carbon content of the sample) curve between the actual operation and the pure pyrolysis. The detailed assessment approach was as follows: if the actual *V*/FC curve sharply went downward and its slope was close to that of the pyrolysis *V*/FC curve, which indicated that the consumption of volatiles *V* was much greater than that of fixed carbon FC, so PC combustion would be in the mode of homogeneous combustion; if the actual *V*/FC curve stayed horizontal or even sloped up, which demonstrated that the consumption of fixed carbon FC was close to or even higher than that of volatiles *V*, so PC combustion would be in mode of heterogeneous combustion; if the actual *V*/FC curve declined slowly, this showed the consumption ratio of volatile *V* to fixed carbon FC fell between the above two cases, so PC combustion would be in the mode of combined combustion.

Considering that the PC for Case 5 and Case 6 is not ignited successfully, only Case 7 and Case 8 were analyzed by the approach introduced above, as shown in Fig. 12.

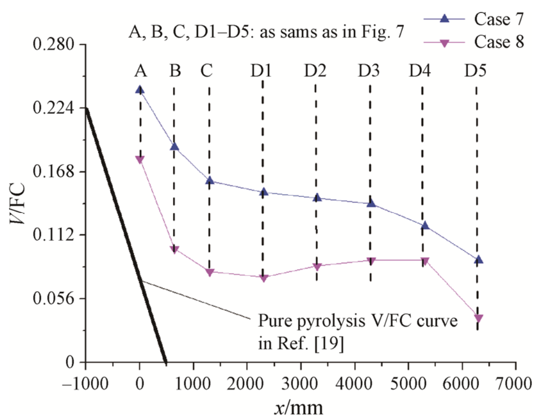

Fig. 12 Evolution of *V*/FC along the center line of combustion chamber

According to analysis method of pyrolysis curve [22], it could be find that in Case 7, the *V*/FC curve could be divided into three parts according to its slope. (1) First part from position A to position C: the actual *V*/FC curve in this part declined rapidly, and its slope was basically close to that of the pyrolysis *V*/FC curve, so PC was in the mode of homogeneous combustion; (2) Second part from position C to position D3: although the actual *V*/FC curve in this part was still downward sloping, its slope was obviously lower than that of the pyrolysis *V*/FC curve, indicating that PC combustion had transformed from homogeneous combustion mode into combined combustion mode; (3) Third part from position D3 to position D5: though being higher than the slope in second part, the slope of actual *V*/FC curve in this part was far less than that of the pyrolysis *V*/FC curve, so the PC was still in the mode of combined combustion. Note that the actual *V*/FC curve presented a slight turn at position D3, which could be explained as follow: the combustion temperature of PC-air flow from position D3 was indeed lower than the ignition temperature of lean coal of 840°C, and such temperature level was qualified to keep volatile component burning strongly, but is not enough to support rapid combustion of the fixed carbon component, thus resulting that *V*/FC curve went down faster.

In Case 8, the *V*/FC curve could be divided into four parts according to its slope. (1) First part from position A to position B: the PC was obviously in mode of homogeneous combustion due to the similarity in slope between the actual *V*/FC curve and the pyrolysis *V*/FC curve; (2) Second part from position B to position C: the actual *V*/FC curve was visibly lower in slope than the pyrolysis *V*/FC curve, indicating that the PC combustion mode was transformed into combined combustion; (3) Third part from position C to position D4: the fact that the actual *V*/FC curve inclined upward showed that a mode of heterogeneous combustion occurred. In such mode, lots of the ignited carbon particles released a large amount of heat to offset the adverse effects of heat loss caused by radiation and convection, keeping PC combustion always in a state of high temperature level, sign of success of PC ignition. (4) Forth part from position D4 to position D5: the actual *V*/FC curve made a turn at position D4 and began to go downward, which meant that PC combustion turned into the mode of combined combustion again.

To sum up, ignition characteristics of lean coal under action of AC plasma arc had been studied experimentally through four cases with different plasma generator power, focusing on the analysis for combustion temperature, combustion regime, carbon burnout rate, and PC combustion mode. The results have revealed that the AC plasma generator power of P=300 kW was a reasonable choice for the lean coal ignition, which could meet the requirements for boiler starting-up.

5. Conclusions

In this paper, a novel AC plasma ignition method was proposed, and the electrode life-span and ignition behavior of lean coal were studied experimentally. The main conclusions were as follows:

(1) A significant decrease in electrode life-span occurred once either cooling water vaporized on the outer surface of the electrode or arcing current was larger than 500 A. Therefore, the AC plasma generator should be operated only under the conditions both that the cooling water flow was large enough to avoid vaporization on the electrode surface and that the arcing current less than 500 A. In this way, the electrode life-span was more than 530 hours.

(2) The PC combustion effect was satisfactory in the condition that the power of the plasma generator was $P_{generator}$=300 kW, which had been proved by experimental phenomena and data, such as the bright flame with a golden color, the average combustion temperature about 940°C, the maximum combustion temperature of 962°C, and the flame length exceeding 6.3 m.

(3) About 80% of cross section of the nozzle outlet was filled with bright flames. Approximate 81% of the PC was in the cylindrical flame regime, while 12% in strip-shape flame regime, indicating that the PC was already ignited at the outlet of the nozzle.

(4) The greatest PC combustion intensity appeared in a region from position C to position D3, where about 27% of the carbon was burned out there. The total burnout rate of carbon reached 52.2% in only 6.3 m long combustion zone, ideal level that can be achieved under experimental conditions.

(5) The PC at initial combustion stage was in homogeneous combustion mode; then it came into the combined combustion mode and heterogeneous combustion mode in turn; at the later stage of combustion, the mode of combined combustion appeared again.

This work proved that AC plasma has advantages in longer electrode life-span and better ignition effect compared with traditional DC plasma, obtaining essential experimental data. This paper contributed to deep understand for PC combustion behavior ignited by AC plasma in specific burner. The results showed that the AC plasma ignition was a promising alternative technology for power plant boilers, especially low-rank coal boilers, achieving the boiler start-up without oil consumption.

Acknowledgements

This work was supported by the national natural science foundation of china (Contract No. 51806132) and doctor start-up capital of Shanxi University (No. 20174462).

References

[1] Liu C.L., Li Z.Q., Kong W.G., et al., Bituminous coal combustion in a full-scale start-up ignition burner: Influence of the excess air ratio. Energy, 2010, 35: 4102–4106.

[2] Yan G.C., Qi X., Ren T., et al., Ignition characteristics of high-temperature oxygen generator in pulverized coal stream. Journal of Harbin Engineering University, 2016, 37: 568–572.

[3] Messerle V.E., Karpenko E.I., Ustimenko A.B., Plasma assisted power coal combustion in the furnace of utility boiler: Numerical modeling and full-scale test. Fuel, 2014, 126: 294–300.

[4] Samuel E.A., Collection efficiency of electrostatic precipitators by numerical simulation. Environment International, 1981, 6: 137–152.

[5] Navarrete B., Vilches L.F., Canadas L., et al., Influence of start-ups with fuel-oil on the operation of electrostatic precipitators in pulverized coal boilers. Environmental Progress, 2004, 23: 29–38.

[6] Liu C.L., Li Z.Q., Kong W.G., Zhao Y., et al., Influence of coal-feed rates on bituminous coal ignition in a full-scale tiny-oil ignition burner. Fuel, 2010, 89: 1690–1694.

[7] Lei C., Fan H.J., Wu L., Numerical simulation on tiny-oil ignition technology for pulverized-coal burners. Journal of Chinese Society of Power Engineering, 2011, 31: 165–169.

[8] Li Z.M., Application of ignition technique with tiny gasified oil for 700 MW subcritical boiler. Boiler Technology, 2015, 46: 65–69.

[9] Yan G.C., Qi X., Ren T., et al., Research on the ignition characteristic of the high-temperature generator in the w-shape flame boiler. Journal of Chinese Society of Power Engineering, 2016, 4: 6–14.

[10] Liu G.W., Dong P., Bie R.S., Experimental study and numerical simulation on high-temperature oxygen-enriched oil-free pulverized coal Ignition. Journal of Chinese Society of Power Engineering, 2013, 11: 833–840.

[11] Yan G.C., Qi X., Ren T., et al., Ignition character of pulverized anthracite coal stream in specific high-temperature oxygen atmosphere. Proceedings of the CSEE, 2016, 36: 1016–1024.

[12] Ju Y., Sun W., Plasma assisted combustion: dynamics and chemistry. Progress in Energy and Combustion Science, 2015, 48: 21–83.

[13] Messerle V.E., Ustimenko A.B., Lavrichshev O.A., Comparative study of coal plasma gasification: Simulation and experiment. Fuel, 2016, 164: 172–179.

[14] Ma J., Zhang M., Su B.G., et al., Numerical simulation of the entrained flow hydropyrolysis of coal in magnetically rotating plasma reactor. Energy Conversion and Management, 2017, 148: 431–439.

[15] Ibrahimoglu B., Yilmazoglu M.Z., Numerical modeling of a downdraft plasma coal gasifier with plasma reactions. International Journal of Hydrogen Energy, 2020, 45: 3532–3548.

[16] Messerle V.E., Ustimenko A.B., Lavrichshev O.A., Plasma coal conversion including mineral mass utilization. Fuel, 2017, 203: 877–883.

[17] Belosevic S., Sijercic M., Stefanovic P., A numerical study of pulverized coal ignition by means of plasma torches in air-coal dust mixture ducts of utility boiler furnaces. International Journal of Heat and Mass Transfer, 2008, 51: 1970–1978.

[18] Zhang H.G., Zhou J.H., Problems and solutions in the application of plasma ignition technology in 660 MW ultra-supercritical units. Journal of Shanghai Electric Power University, 2016, 32: 84–86.

[19] C.Y. Han, Xu M.H., Zhou H.C., et al., Pulverized coal combustion, sixth, ed., Science Press, Beijing, 2001, pp.: 309–325.

[20] Costa M., Silva P., Azevedo J.L.T., Measurements of gas species, temperature, and char burnout in a low-NO_x pulverized-coal-fired utility boiler. Combustion Science and Technology, 2003, 175: 271–289.

[21] Hwang J., Bae C., Park J., et al., Microwave-assisted plasma ignition in a constant volume combustion chamber. Combustion and Flame, 2016, 167: 86–96.

[22] Fang C.Q., Jiang X.G., Lv G.J., et al., Chemical synthesis residual pyrolysis and combustion: kinetics and evolved gases investigated by TG-FTIR. Journal of Thermal Science, 2020, 29(1): 108–114.